Polymer Chemistry

Visible Light-Induced Controlled Surface Grafting Polymerization of Hydroxyethyl Methacrylate from Isopropylthioxanthone Semipinacol-terminated Organic Monolayers

Journal:	*Polymer Chemistry*
Manuscript ID	PY-ART-10-2020-001410.R1
Article Type:	Paper
Date Submitted by the Author:	11-Dec-2020
Complete List of Authors:	Balasubramaniam, Ajitha; Ruhr-Universität Bochum Manderfeld, Emily; Ruhr University Bochum, Krause, Lutz; Ruhr-Universität Bochum Wanka, Robin; Ruhr-Universitat Bochum, Schwarze, Jana; Ruhr-Universität Bochum Beyer, Cindy; Ruhr University Bochum, Rosenhahn, Axel; Ruhr-University Bochum, Analytical Chemistry - Biointerfaces

Visible Light-Induced Controlled Surface Grafting Polymerization of Hydroxyethyl Methacrylate from Isopropylthioxanthone Semipinacol-terminated Organic Monolayers

Ajitha Balasubramaniam‡, Emily Manderfeld‡, Lutz M. K. Krause, Robin Wanka, Jana Schwarze, Cindy Beyer, and Axel Rosenhahn*

Analytical Chemistry – Biointerfaces, Ruhr University Bochum, 44780 Bochum, Germany

‡ These authors contributed equally to this work.

* Correspondence email: axel.rosenhahn@rub.de

1 Abstract

A visible light-induced living polymerization of a hydrophilic model monomer was initiated on organic silane monolayers using isopropylthioxanthone (ITX). The type II photoinitiator ITX was covalently introduced to the octadecyltrichlorosilane monolayers by UV-induced (254 nm) hydrogen abstraction and a subsequent coupling step through recombination. The resulting dormant isopropylthioxanthone-semi pinacol (ITXSP) groups can be reactivated by irradiation with visible light to initiate a controlled surface grafting polymerization. Using this surface-initiated polymerization approach, hydroxyethyl methacrylate (HEMA) was polymerized under visible light irradiation (385 nm) at room temperature. The polymer layer thickness depends linearly on the irradiation time, which is in good agreement with previous reports on the living characteristics of the polymerization reactions. It is possible to accurately control the thickness of the grafted layer by simply altering the irradiation time.

Keywords: pHEMA, isopropylthioxanthone, type II photoinitiator, *Navicula perminuta*, photo patterning, living polymerization, surface grafting

2 Introduction

In recent years, the synthesis of polymer brushes played a decisive role in the controlled modification of surface properties. Synthetic control over polymer brush growth allows to tailor surfaces to specific needs by the application of a variety of monomers with various functional groups. Surface-initiated polymerization is known as the direct polymerization from initiating sites at the surface.(1–5) There are three well-known and established controlled radical polymerization mechanisms: the dissociation-combination mechanism, generally known as stable free radical polymerization, but often only referred to the nitroxide-mediated radical polymerization, the bimolecular activation, represented by the atom transfer radical polymerization (ATRP), and the degenerative transfer, carried out through the reversible addition-fragmentation chain transfer method (RAFT). These controlled free-radical polymerization techniques involve surface pre-functionalization to create active sites that can be used for a subsequent, surface-initiated polymerization. In contrast to free radical polymerization, controlled radical polymerization is characterized by an initiation rate higher than the growth rate, the absence of chain termination and transfer reactions, infinite live times of the active chains resulting in polymerization reactions until depletion of the monomer, the opportunity of block copolymer synthesis and narrow molecular weight distributions.(6–13)

Conventional surface initiated free radical polymerization has the advantages of an effortless operation, low cost, mild reaction conditions and avoidance of negative effects on the bulk polymer.(14–17) For this procedure, the photoinitiator benzophenone has been frequently used. Also thioxanthone and its derivatives are widely used conventional photoinitiators for technologically important UV-curing applications, because of their excellent light absorption characteristics.(25–28) Nevertheless, less control over the growth of the polymer chains to obtain uniform, homogenous brushes and the reactivation of the polymer chains is a problem.(18) For the formation of grafted block polymers, reactivation of the dormant group terminating the polymer chain is necessary.(19)

For this reason, Yang and Ranby(5) invented a two-step “living” photografting process, which is based on a photoinitiation mechanism and was subsequently further developed into a sequential system which had a 4-fold greater amount of grafted polymer relative to the total amount of polymer compared to the simultaneous grafting method.(20, 21) The idea consists of using a previously developed “living radical polymerization” based on the covalent coupling of a stable free radical for reversible deactivation of growing radicals. The process can be exploited for surface-grafting polymerizations. This surface grafting has the advantage over solution and bulk polymerization, that the growing radicals are predominantly located on the solid surface due to the covalent connection of the ITXSP to the surface. This results in low mobility, and the low free radical concentration, which favors the surface-induced “living” polymerization reaction.(5) In order to form the ITXSP on the

surface, ITX in solution is irradiated with UV light in the presence of the substrates. After hydrogen abstraction, the semi pinacol end groups are formed, which serve as “dormant” groups on the surface of the organic substrate (e.g., model films like glycidyl methacrylate or low-density polyethylene). In the second step, the “living” polymerization was initiated by the reactivation of the dormant groups.(5, 15, 22, 23)

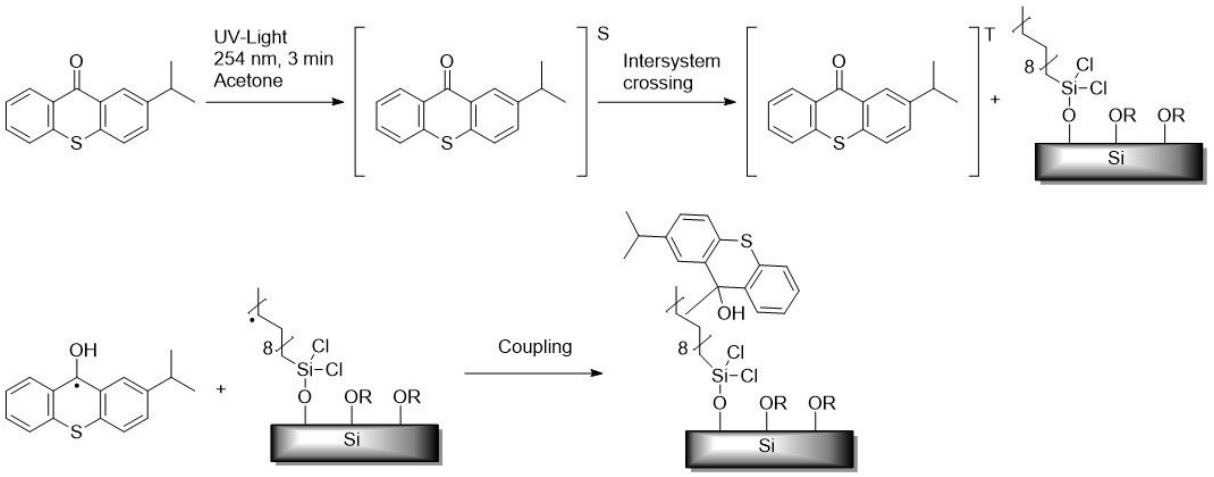

Figure 1: Reaction scheme of the introduction of the dormant ITXSP group using a photoreduction reaction. Excitation with UV light to singlet state and relaxation to triplet state. After hydrogen abstraction from the alkyl chain of OTS the coupling occurs and a dormant ITXSP group is formed.

The use of isopropylthioxanthone semipinacol (ITXSP) for visible light-induced (in the range of 380 to 420 nm) “living” polymerization reactions is only described for few surface-induced photografting applications. As reported in literature, ITX can readily be immobilized on polymer surfaces(5, 23, 24) with the according mechanism schematically shown in Figure 1. The dormant terminal groups can be introduced to the surface through UV irradiation (254 nm). Under UV irradiation, ITX is excited to the singlet state (ITX^S) and instantaneously relaxes to the stable triplet state (ITX^T) via intersystem crossing, which can abstract a hydrogen atom from the surface of the OTS monolayer. The ITXSP radicals undergo recombination reactions with the freely accessible surface radicals to form the dormant ITXSP groups.(21)

The thickness of grafted polymer brushes can be controlled by the growth conditions like temperature, irradiation time, monomer, and the interfacial grafting density of isopropylthioxanthone semi pinacol (ITXSP). Furthermore, the controlled, light-sensitive character of ITXSP-induced polymer growth provides the opportunity to control the vertical brush architecture by the creation of block copolymers through chain reactivation in different monomer solutions and to control the horizontal distribution of brushes by using photomasks with patterns during irradiation.(24, 29, 30)

Visible light based systems present several advantages over UV-induced polymerization reactions, such as safety in biomedical applications, avoidance of UV-induced damages to the polymers, larger penetration depth through solvents, and the applicability to pigmented systems where UV penetration and scattering concerns.(27, 31, 30) For example Ziani-Cherif *et al.* used visible light-induced surface grafting polymerization to modify the inner surface of a transparent segmented polyurethane (SPU) artificial heart device.(32) Furthermore, Magoshi and Matsuda used this technique to form a densely packed heparin- or albumin-polymerized surface layer using camphorquinone (CQ) as the initiator and SPU films as the substrate for tissue-engineered devices.(33) In recent years, visible-light-induced grafting polymerization by dormant ITXSP groups was frequently applied to incorporate or immobilize enzymes like papain and cellulase into or onto polymer films proving the broad scope of possible applications. (34–37)

Based on the great potential that visible light-induced controlled polymerization reactions offer, the aim of this work was to develop a versatile platform for controlled surface functionalization using a variety of monomers and subsequent antifouling tests. Instead of starting the reaction from the surface of bulk polymers, we used OTS as thin organic monolayer substrate that can be applied easily to numerous organic and inorganic surfaces, thus working as a uniform and universal link. ITX was then photoimmobilized on the coating to form the dormant ITXSP groups. These coated surfaces can then be used for a visible light-mediated, controlled surface grafting polymerization at room temperature which was exemplarily shown using HEMA as methacrylate monomer. The obtained brushes were characterized by state-of-the-art surface analysis like spectroscopic ellipsometry, contact angle goniometry, attenuated total reflection-Fourier-transform infrared spectroscopy (ATR-FTIR), atomic force microscopy (AFM) and scanning electron microscopy (SEM). The obtained HEMA coatings were then tested regarding their resistance against the adhesion of marine diatoms as model biofilm-forming organisms. Challenging the feasibility of the system, micro-structured patterns were polymerized using photomasks.

3 Experimental Section

3.1 Chemicals and Substrates

Acetone p.a. (Sigma-Aldrich, ≥ 99,5 %), chloroform (Fischer Chemicals, ≥ 99.8 %), cyclohexane (Fisher Chemicals, ≥ 99.99 %), ethanol (Roth, ≥ 99.8 %, p.a.), toluene (Fisher Chemicals, ≥ 99.98 %) were used as received. Octadecyl trichlorosilane (≥ 90 %) was purchased from Sigma-Aldrich and not purified. The received bottle was only opened in a glovebox to ensure a water-free atmosphere and to avoid hydrolysis. 2-Isopropylthioxanthone (ITX, 98.0 %) was bought from TCI, recrystallized once from ethanol, and stored at -20 °C. Hydroxyethyl methacrylate (HEMA, Sigma Aldrich chemical ≥ 99.8 %) was used as received. Distilled water was purified by an Milli-Q-Plus system (Siemens). Silicon wafers (<100> orientation, 100 mm diameter, 525 µm thickness, prime quality) were obtained from Siegert Wafer (Aachen, Germany). Nexterion B® (clean room cleaned) glass slides were obtained from Schott (Jena, Germany). All substrates were stored under an argon atmosphere.

3.2 Light Sources for Photochemistry

For the coupling of ITX to the organosilane monolayers, a 254 nm UV light source Osram Sylvania G8T5 (8W G5 288 mm T5, 15 W) was used. For the visible light-induced controlled photopolymerization, an LED system with a 385 nm LED (NVSU233A-D1 U385; Nichia Corporation, Japan; 1 A, 3.65 V, 385 nm peak wavelength, 11 nm spectrum half width, 1400 mW radiant flux, 60° viewing angle, relative radiant intensity of 1 within ± 10° radiation angle and ≥ 0.9 within ± 40° and an irradiation intensity of 72 mW/cm^2) was used. The necessary cooling for the high-power UV LED was achieved assembling it to an EK Water Blocks EK-Supremacy MX processor water cooler.

3.3 Contact Angle Goniometry

The static water contact angles (WCAs) were measured using a custom-built goniometer. The water droplets (≈ 50 µL) were deposited on the sample surface and their shapes were recorded via a charged coupled device camera. The implemented contour tracing algorithm automatically distinguished between drop and mirror image. The shape analysis was accomplished using Young's equation. The presented values were obtained on at least three replicates and three measured positions. The error bars represent the standard error.

3.4 Spectroscopic Ellipsometry

The film thickness was determined by spectroscopic ellipsometry. Measurements were carried out using a M-2000 V (J.A Woolam, Lincoln, USA) which measures in the spectral range between 370 and

1000 nm. All measurements were carried out at three different incidence angles (65°, 70° and 75°). The film on the surface was modeled as single organic layer with a wavelength-dependent refractive index described by a Cauchy model (A = 1.45, B = 0.01, C = 0). We used the software package CompleteEASE Version 4.98 for data analysis. Data obtained from at least three independent measurements on three replicates per chemistry was averaged to determine the thickness. The error bars represent the standard deviation.

3.5 Attenuated Total Reflection-Fourier Transform Infrared Spectroscopy

The ATR-FTIR spectra (VariGATR, Harrick, USA) were obtained with a Bruker Tensor 27 spectrometer (Ettlingen, Germany), with a liquid N_2-cooled MCT detector. Before measuring the first spectra the system was purged with nitrogen for 30 min. As background the spectrum of the Ge-ATR crystal was used. The background was measured with 50 scans and the samples with 150 scans (2 cm^{-1} resolution).

3.6 Atom Force Microscopy and Scanning Electron Microscopy

The AFM images were obtained using a NanoWizard 3 (JPK, Germany) controlled by a Vortis control station III. For tapping mode, an OTESPA-R3 (300 kHz) cantilever (JPK, Germany) was used. Typical settings for a 100x100 µm scan area are 4V target amplitude, 2 V setpoint, 150 Hz igain, and 112 µm/s tip velocity. The SEM images were obtained using a Quanta 3D FEG (FEI Company, Hillsboro, OR, USA) Typically settings were 10 kV and a 4.5 spot size.

3.7 UV/Vis Spectroscopy

UV/Vis spectra were recorded in an Agilent Cary 60 spectrophotometer. The measuring range was between 200 and 600 nm. The scan rate was 600 nm/min. A blank Nexterion B slide was used for the background measurement.

3.8 Preparation of OTS Monolayer

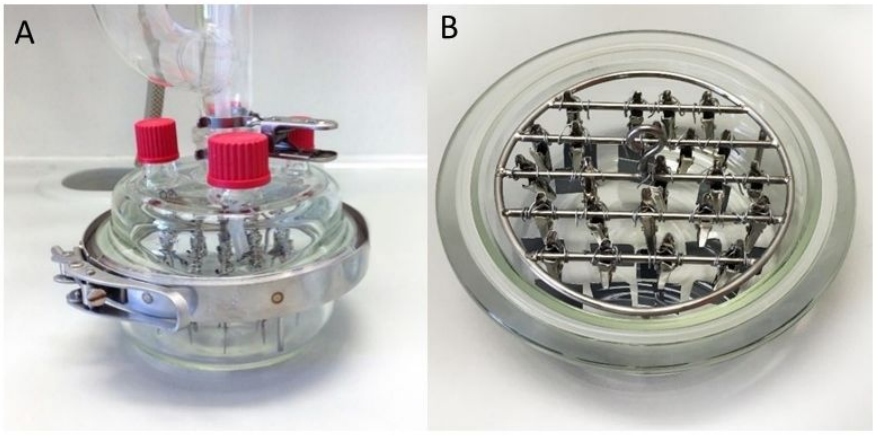

Figure 2: Silanization reactor for the synthesis of OTS-coated silicon substrates. (**A**) Silanization reactor equipped with a two-neck ground glass joint connected to a tap (nitrogen flow) and a plug-sealed dropping funnel and (**B**) bottom assembly of the reactor with frame and clamped silicon surfaces.

The silicon wafers were cleaned from silicon particles and dust through a nitrogen jet and immediately stored in a clean petri dish to avoid dust contamination. The petri dish was inserted into a GaLa miniFlecto MFC plasma cleaner (argon oxygen plasma, 0.4 mbar, 80 W, 22 kHz, 3 min) for both plasma cleaning through removal of organic contaminants (oxygen plasma), physical ablation (argon plasma), and plasma surface activation through surface oxidation and hydroxylation (oxygen plasma). Under inert conditions, OTS was transferred to 5 ml borosilicate glass bottles, which were sealed and stored at -20 °C until further use. Synthesis was carried out in a silanization reactor, which is shown in Figure 2. It is a desiccator-shaped borosilicate glass reactor with a NS 29 ground glass joint and four screw-cap joints. The NS 29 ground glass joint were equipped with a two-neck ground glass joint (3 x NS 29), which is connected to a NS 29 ground glass joint tap for a nitrogen flow and a 500 ml dropping funnel (2 x NS 29) sealed with a plug and connected to a Teflon hose directing the dropping funnel content to the reaction space. Additionally, a V2A frame with holding clips was placed in the reactor. The clips were used to hold the plasma-activated silicon surfaces and, under an argon atmosphere, 350 µl OTS were mixed with 350 ml of the solvent mixture (75 % cyclohexane, 25 % chloroform (v/v)) in the dropping funnel and added to the reactor. The sealed reactor was sonicated (Bandelin Sonorex Super, 35 kHz, 480 W) for 30 min at 10-15°C. After the silanization process was finished the samples were removed from the reactor, placed in covered crystallizing dishes filled with cyclohexane and toluene and sonicated for 3 min each time and dried in a stream of nitrogen.

3.9 Photografting of “Dormant” ITXSP Groups on Si-OTS films by UV Irradiation

A 0.5 M solution consisting of ITX solved in acetone was placed in a Schlenk tube and three times degassed using the freeze-pump-thaw method to remove oxygen. Subsequently, Si-OTS surfaces were immersed into a Schlenk tube and exposed to 254 nm UV light (Osram Sylvania G8T5 8W G5 288 mm T5, 15 W) for 3 minutes. After irradiation, the modified surfaces were rinsed with acetone and sonicated in acetone for 30 min to remove the adsorbed, but not covalently attached ITX.

3.10 Visible Light-Induced Surface Grafting Polymerization on Si-OTS-ITXSP

The polymerization was carried out in solutions of 0.1 w%, 0.2 w%, and 0.5 w% HEMA in acetone. These solutions were degassed three times using the freeze-pump-thaw method to remove oxygen. Si-OTS-

ITXSP surfaces were placed into the solution in a Schlenk tube. The distance between the light source (385 nm LED) and the substrate was fixed to 3 cm and the Schlenk tube was irradiated for the desired time. After the polymerization reaction was completed, samples were retrieved, placed in degassed acetone for 24 h to leach out all uncoupled monomer and dried in a stream of nitrogen.

3.11 Removal of ITXSP Groups

To remove the dormant ITXSP groups, acetone was purged for 15 min with oxygen and the surfaces (Si-OTS-ITXSP-, Si-OTS- pHEMA-ITXSP) were immersed into the acetone in a Schlenk tube. The surfaces were irradiated for 10 min by the 385 nm LED. Afterwards the surfaces were immersed into an acetone bath to leach for further 24h.

3.12 Surface Patterning by Visible Light-Induced Surface Grafting Polymerization

For this step, a custom made holder was designed which is shown in Figure . The head of the stamp has two cavities. The distance between these two cavities is about 3 mm. A TEM Grid (Plano GmbH, Wetzlar, Germany; hexagonal structure copper 400 mesh with 10 - 12 µm thickness) was placed in the holder (b) and covered by small pieces of OTS-ITXSP-coated silicon (1.5 mm^2). As the TEM grid fitted into the recession of the holder (b), the grid was not in direct contact to the silicon and only shaded defined parts of the LED beam. The holder was closed by screwing in part (a) and the assembly was immersed into a Schlenk tube filled with 0.5 w% HEMA solution. The Schlenk tube was placed 3 cm above the LED lamp for photopatterning.

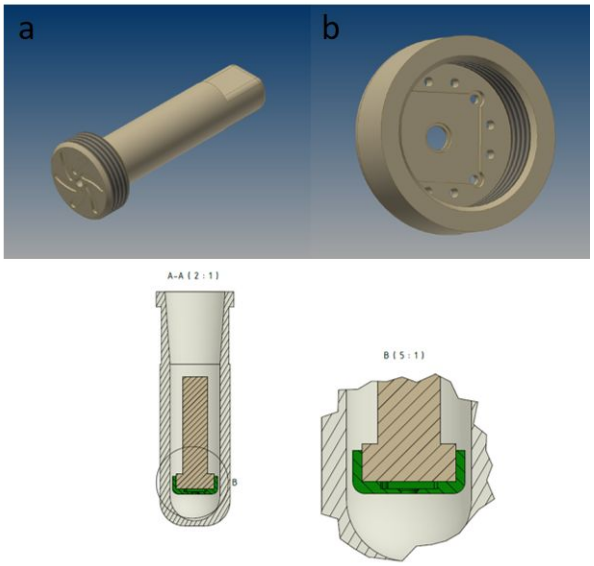

Figure 3: Schematic illustration of the sample holder used for patterning. It consists of the holder illustrated in (b) and the lid that keeps the TEM-grid / silicon assembly in place (a). The central round recession is used for the TEM Grid and the IXTSP coated silicon is placed into the rectangular recession. The part above the small holes in the bottom of the sample holder allow the monomer solution to enter the cavity and to completely cover the silicon. The assembly is made of polyether ether ketone with a total size of 45 mm and a thickness of 10 mm (upper part) / 16.42 mm (lower part). The recession for the silicon wafer is 9.2 x 9.2 mm and the hole for the TEM grid 3.1 mm with a height of 0.3 mm. See Figure S1 for a technical illustration.

3.13 Stability Test

The stability of the prepared surface coatings was tested in salt water (SW), containing the seven most abundant salts (> 50 ppm) of the recipe of Kester(38) for artificial seawater over 28 days. The samples were immersed in SW on an orbital shaker (60 rpm) for the selected duration and subsequently rinsed with water and dried in a stream of N_2. The thickness of the coatings was determined by spectroscopic ellipsometry and ATR-FTIR spectra were measured after immersion.

3.14 Microfluidic Diatom Accumulation Assay

Diatom culture and the microfluidic accumulation assay followed previously published protocols.(39, 40) The diatom *Navicula perminuta* was used as a model organism. For the assay, the culture medium was exchanged for filtered seawater (FSW pH 8), and a total cell concentration of 2 million/mL was adjusted using OD_{444}. The microfluidic experiment was performed on polymer-coated Nexterion B glass slides and on OTS-coated slides as a nonresistant control to account for slight variations in the physiological state of the diatoms. Sticky slides 0.1 (IBIDI, Germany) were glued onto the samples and formed the channel system. For each coating, three accumulation assays were conducted at a constant wall shear stress of 0.18 Pa over 90 min. To remove any unattached diatoms, pure FSW was rinsed

through the channels at the same speed as for the accumulation assay for 10 min. Thirty fields of view (each 0.757 mm^2; 1004 µm × 754 µm) in the middle of the channel were recorded using an inverted video microscope (Nikon Ti-E, Nikon Japan; 10× phase contrast objective Nikon CFI Plan Fluor DLL NA 0.3, Nikon Japan).

4 Results and Discussion

4.1 Introduction of ITXSP onto Si-OTS films by UV Irradiation

To create pHEMA brushes, several synthesis steps were required as illustrated in Figure 1. In the first step, an OTS monolayer was assembled on the plasma activated substrate in solution. The prepared OTS monolayers were characterized by spectroscopic ellipsometry and contact angle goniometry. An average film thickness of 2.6 ± 0.1 nm and an average contact angle of 110° ± 3° were determined and indicated the successful formation of the silane layers (Table 1).(41)

Table 1: Surface analysis of the plasma treated silicon substrate (Si-OH), the OTS-coated silicon (OTS), and layer thickness on top of the OTS monolayers for the different ITX and monomer concentrations. Static water contact angles were determined by contact angle goniometry and film thicknesses by spectroscopic ellipsometry. Plasma activated Si-OH and the assembled OTS layers are shown in comparison to the pristine silicon. ITXSP adlayers were attached at different ITX concentrations, the thickness increase on top of the OTS was calculated, and contact angles were determined. The properties of the pHEMA brushes were analyzed after 10 min of polymerization with different HEMA monomer concentrations. The thicknesses refer only to the thickness of the polymer brushes on top of the OTS-ITX. The standard deviation (n=3) is given as the error.

	Monolayer		ITX			HEMA		
	Si-OH	OTS	0.1M	0.3M	0.5M	0.1 wt%	0.3 wt%	0.5 wt%
Contact angle / °	< 10	110 ± 3	108 ± 1	103 ± 1	76 ± 3	56 ± 3	52 ± 3	48 ± 2
Adlayer thickness / nm	±0	2.6 ± 0.1	±0	0.3 ± 0	0.7 ± 0.2	8 ± 2	16 ± 2	50 ± 5

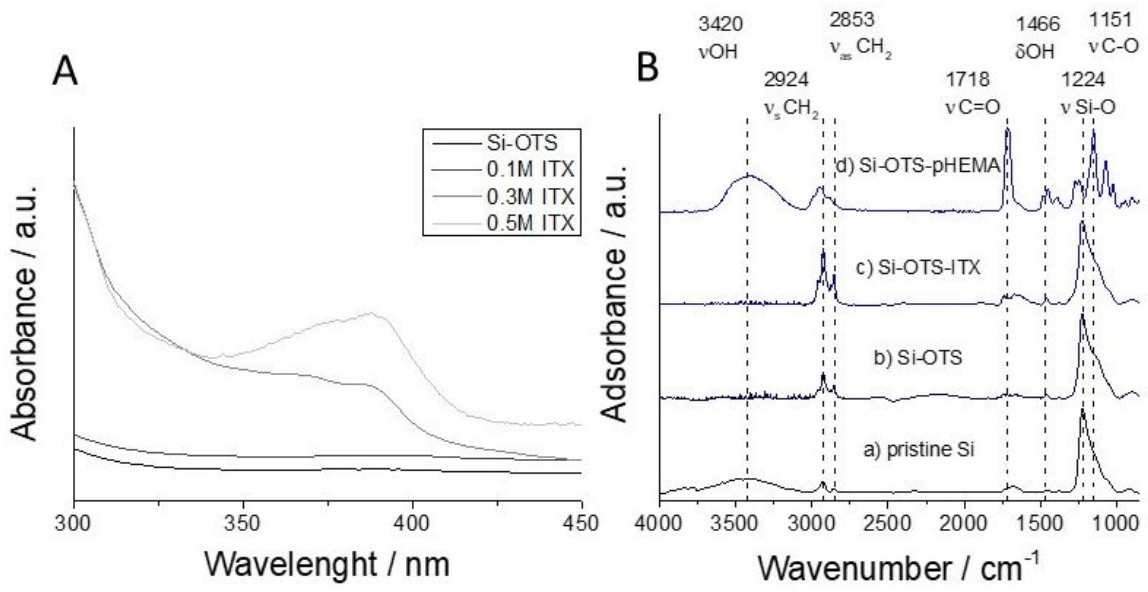

Figure 4: A: UV/Vis spectra of glass slides coated only with an OTS monolayer (Si-OTS) and dormant ITXSP groups on OTS coupled at different ITX concentrations. The irradiation time was 3 min using the 254 nm UV LED for the ITX coupling step. **B:** ATR-FTIR spectra of the pristine silicon (a), the OTS coated silicon substrate (b), the ITXSP-functionalized OTS surface (c), and Si-OTS-pHEMA surface (d).

The second step was the covalent introduction of dormant ITXSP groups on the OTS monolayer. To verify the successful formation of dormant ITXSP groups on OTS, samples were characterized by UV/Vis and ATR-FTIR spectroscopy. The pristine OTS surface showed no absorption bands in the UV/Vis spectra while UV/Vis spectra of the ITXSP functionalized samples in Figure 4A exhibited an absorption peak at about 390 nm. As expected, the UV/Vis absorption of the ITXSP coatings increased with the ITX concentration in the coating solution and thus a ITX concentration of 0.5 M showed stronger absorption bands than coupling with an ITX concentration of 0.3 M. An ITX concentration of 0.1 neither showed a relevant change in thickness, nor CA or UV/Vis signals, indicating that insufficient coverages were reached (Table 1). Either the amount of coupled ITX was below the detection limit or radicals could have been inhibited by impurities or molecular radical interceptors (e.g., O_2, NO). Amirzadeh and Schnabel,(25) Allen *et al*.(42) and Corrales *et al.* have also reported similar results involving ketyl radicals with a characteristic absorption in the region of 380 - 420 nm. Table 1 shows the change in contact angle and the increase in thickness after ITXSP was coupled to the OTS monolayers at different ITX concentrations. The ITXSP-coupling at a concentration of 0.3 M caused a minor decrease of the CA from 110° to about 103° and a slight increase in thickness. The CA decreased even more at a concentration of 0.5 M ITX. The ellipsometry data also underlined a successful ITXSP coupling (0.7 ± 0.2 nm) which corresponds very well with the absorption band in the UV/Vis spectra. After immersing the surfaces several times in acetone, the contact angle and the UV/Vis spectra remained unchanged. This suggests that the ITXSP was successfully covalently grafted onto the OTS monolayers.

ATR-FTIR spectroscopy was used to further prove the different coupling steps to the surface. The spectra are shown in Figure 4B. The ATR-FTIR spectrum of the pristine silicon substrate (a) revealed only a peak at 1220 cm^{-1} that can be assigned to the stretching vibration of the Si–O–Si. The spectrum of the OTS monolayer (b) exhibited the typical aliphatic asymmetric stretching vibration of the methylene groups $\nu_{as}(CH_2)$ at 2925 cm^{-1} and the symmetric ones $\nu_s(CH_2)$ at 2851 cm^{-1}.(43) The spectrum of the Si-OTS-ITXSP surface (c) reveals a hydroxyl deformation vibration (δ OH) as result of the successful ITXSP coupling. The C-H stretch vibrations from the aromatic system of ITX, which usually occur between 3066 cm^{-1} and 3028 cm^{-1}, are visible as a shoulder around 3000 cm^{-1}.

4.2 Visible Light-Induced Grafting Polymerization on Si-OTS-ITXSP and Deprotection

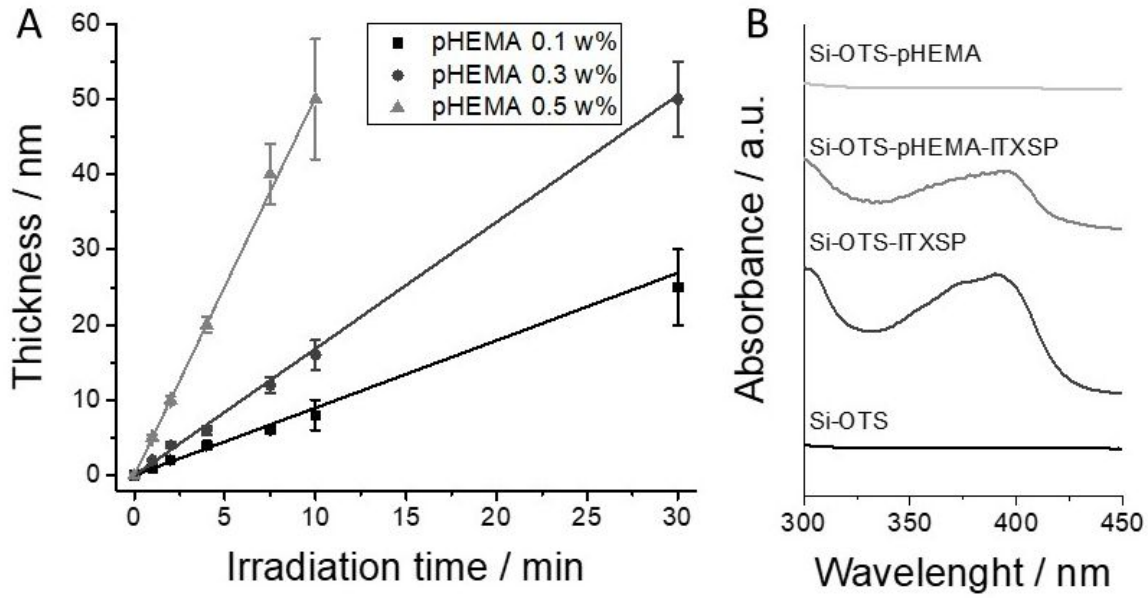

Figure 5: pHEMA brush formation on the Si-OTS-ITXSP surfaces. (A) Polymer brush thickness for different irradiation times and for three different concentrations of HEMA in acetone. Each point represents an independent sample. The irradiation intensity was 72 mW/cm^2 (B) UV/Vis spectra of the Si-OTS monolayer and after ITXSP coupling leading to a spectrum that exhibits a peak around 385 nm which belongs to the covalently bound ITXSP. This peak is also present in the pHEMA-ITXSP after polymerization but vanishes after decoupling.

It was proven earlier that the surface bound ITXSP can be photoactivated and a radical is liberated which is capable to react with methacrylate monomers in solution. After the capture of the methacrylate monomer, the free radical is protected again by the ITXSP until it gets photoactivated again (24, 23, 5). Here, the ITXSP bound to OTS is used to prepare HEMA polymer brushes. Figure 5A shows the increase of the layer thickness with irradiation time for different HEMA concentrations (0.1, 0.3 and 0.5 w%). Each data point represents an independent sample. While the linear dependence on

irradiation time and concentration is only an indication and not a proof of the livingness of the polymerization reaction. Latter can be proven by the possibility to restart the reaction as described by Stenzel *et al.(44)*. As shown in the Supplementary Information, the restart of the polymerization is possible for the OTS-ITXSP system even after removing the sample from the methacrylate solution and reimmersion into a different monomer solution (Table S1). The successful copolymerization was proven by the increase in layer thickness as well as the change in wettability. This result is in agreement with literature, where not only the restart was tested, but also the kinetics of the "living" polymerization with ITX or benzophenone was characterized in detail (5, 20, 45). With higher monomer concentration, a faster increase in layer thickness was detected (Figure 5a). At a concentration of 0.5 w%, the fastest polymerization rate of 7 nm/min was observed. At 0.1 w% the lowest thickness increase rate of 1.5 nm/min was detected.

As shown in Table 1, the water contact angles show the expected decrease after the growth of the pHEMA brushes and reach values <60°. Figure 4B shows the ATR-FTIR spectra of the pHEMA brushes and an enhanced hydroxyl peak at 3200 – 3600 cm^{-1} appeared. In the carbonyl region, a distinct peak at 1714 cm^{-1} was found which is caused by the carbonyl stretching vibrations of esters as occurring in pHEMA. The strong band at 1140 cm^{-1} can be assigned to the ether stretching vibration of the pHEMA. The film thickness increase, water contact angle change, and the ATR-FTIR spectra prove that pHEMA brushes are successfully grafted from the surface.

As the ITXSP groups terminate the chain again after the addition of each new monomer (46), ITXSP groups are still present on the surface at the end of the polymerization reaction. A proof of this observation has been shown by the possibility to restart the reaction after retrieval of the sample as shown in the Supplementary Information and in several publications (24, 46). In all cases, the polymerization can be simply reactivated by irradiation of the polymer brush in a different, oxygen-free monomer solution as long as the ITXSP is terminating the polymer brushes.

As the presence of ITXSP groups at the surface could influence the antifouling effects, it was important to remove the photoinitiator after the polymerization reaction has been completed.(47) The removal of the dormant ITXSP groups was realized by irradiating the surfaces with visible-light (385 nm LED) in an oxygen-containing solution. The peroxide radical grown by addition of molecular oxygen is an unreactive radical in comparison to methacrylate radicals and can either terminate the polymer chain by rearrangement to a ketone and an alcohol or transfer the radical center to another chain by abstraction of a hydrogen atom. The successful cleavage of the ITXSP was shown by UV-Vis spectroscopy (Figure 5B). Si-OTS films prior to coupling the ITX showed no absorption bands in the

UV/Vis region. The Si-OTS-ITXSP surfaces revealed the expected peak at a wavelength of about 390 nm which was maintained during the pHEMA brush formation (Si-OTS-pHEMA-ITXSP). The successful deprotection of the ITXSP from the Si-OTS-pHEMA film becomes obvious as the ITXSP peak disappeared completely after 10 min irradiation time. In addition, no further polymerization was observed under the same polymerization conditions after ITX removal. Those results are in agreement with previous studies (24) , which show the "living" ITXSP terminal groups of poly(EGMA) brushes toward further photo-assisted polymerization indicating that the ITXSP groups present at the surface are still accessible to initiate further grafting.

4.3 Photopatterned polymer brushes

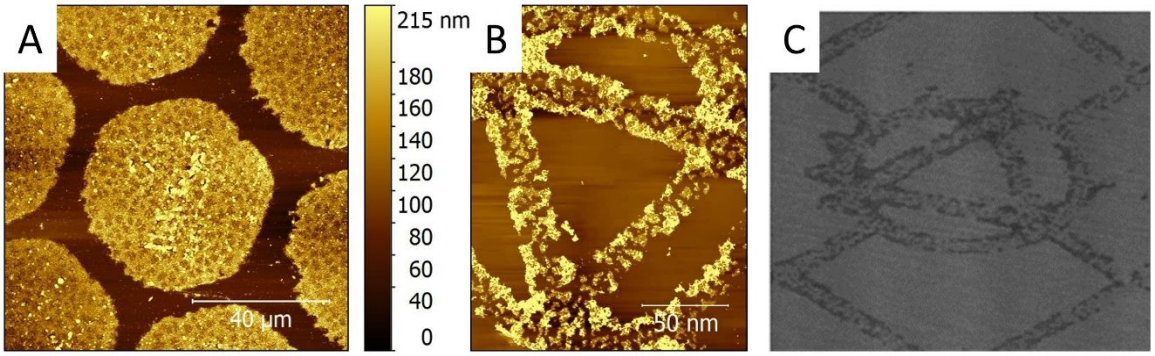

Figure 6: Photopatterning of pHEMA polymers using visible light (λ=385 nm). AFM images of honeycomb structures (A) and letters (B) patterned by photo induced polymerization of HEMA using TEM grids as masks. (C) SEM image of the photopatterned structures.

Among the advantages of using visible light to induce the photografting process is the possibility to use masks to locally grow polymer brushes to create patterned surfaces. As a proof of principle, we used TEM grids as photomask and illuminated them with a collimated light cone with a wavelength of 385 nm. In order to obtain sharp edges, the distance between the TEM grids and the Si-OTS-pHEMA-ITXSP functionalized substrates, a custom build holder was designed as described in the materials and methods section and the Supplementary Information. Figure 6A shows honeycomb like structures and 6B shows a letter-like triangle which were polymerized at the specific locations due to the localized irradiation through the TEM grid. The structured illumination leads to a local polymerization of the HEMA and opens the possibility to create even more complex patterns consisting of different chemistries if the monomer solution is exchanged. Among the applications of structured polymer surfaces is their use in studying the response of biological organisms to surface patterns as it was done in the case of hierarchically wrinkled pHEMA which was tested against marine fouling species.(48)

4.4 Stability Test and Microfluidic Diatom Accumulation Assay

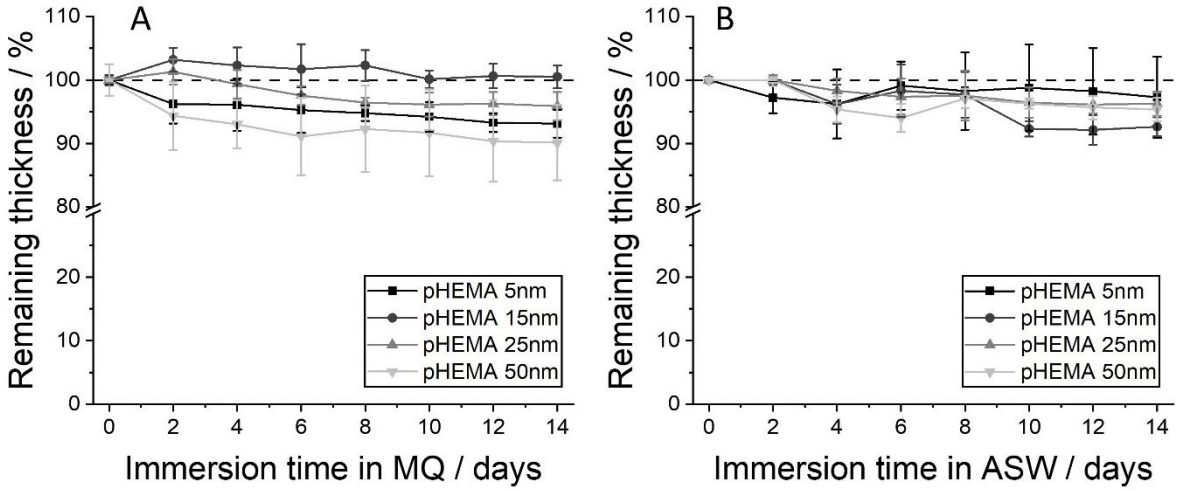

Figure 7: Remaining thickness of the pHEMA coatings of different thickness for different durations in MQ (**A**) and in ASW (**B**). Thicknesses were determined by spectroscopic ellipsometry. Reported values are the average of three independent measurements, error bars represent the standard deviation.

To ensure that the coatings are stable for the duration of the biological experiments we investigated the stability of the surfaces in MQ (A) and ASW (B) by incubating the surfaces for up to 14 days. The thickness was measured by spectroscopic ellipsometry after different immersion times. Figure 7 shows that the overall thickness for all four coatings changes in both cases by <20% over the period of the 2 weeks, proving the necessary stability in aqueous media.

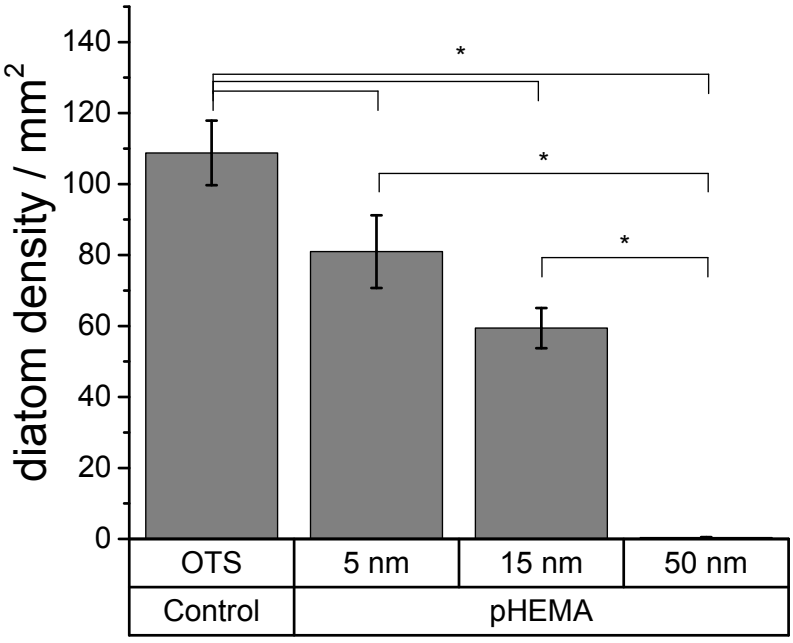

Figure 8: Settlement of the diatom *N. perminuta* on pHEMA brushes of different thickness. Average diatom density was determined in 30 fields of views across the surface. The data shown are the merged data from three

independent measurements, error bars represent the standard error. A one-way ANOVA with post-hoc Tukey test (*, significance level of $\alpha = 0.05$) revealed differences that are statistically significant.

Using a custom-built parallel microfluidic setup, we tested the marine antifouling properties of three different layer thicknesses of pHEMA and compared it to the hydrophobic, negative OTS control. *N. perminuta* was chosen as a model organism because of its ubiquitous presence in the oceans. The results reveal that OTS has significantly higher attachment of diatoms (109 ± 9 diatoms/mm^2) than the hydrophilic pHEMA (Figure 8). While lower thicknesses of pHEMA (5 and 15 nm) showed a moderate reduction in diatom densities (81/59 diatoms/mm^2), higher thickness of HEMA suppressed diatom attachment effectively. Brushes with 50 nm thickness reduced the settlement to 0.4% (1 diatoms/mm^2) compared to the negative OTS controls. The statistical significance of the observed differences in diatom densities was determined by a one-way ANOVA with post-hoc Tukey test (significance level of $\alpha = 0.05$). OTS has significantly higher settlement than all other tested coatings. Also, the antifouling performance of the different thicknesses of HEMA is statistically significantly different from the densities on 5 nm and 15 nm pHEMA coatings ($\alpha = 0.05$.) The results clearly show that higher polymer thicknesses are more effective in reducing diatom attachment.

Our results are in line with literature describing HEMA as a powerful co-monomer for antifouling coatings.(49, 50) The thickness dependence observed in our experiments is in excellent agreement with previous reports on the inert properties of pHEMA polymer brushes synthesized by Si-ATRP on silicon.(51) Both, settlement of diatoms and green algae, was significantly reduced when the thickness of the pHEMA brushes was increased. In coherence with our experiments brush thicknesses of 55 nm strongly reduced settlement to very small densities. Kim *et al* developed a ternary system with styrene, ethylene glycol methacrylate (EGMA) and HEMA and tested their protein resistance showing that polystyrene (pS)/pHEMA performed considerably worse than pS/pEGMA or pS-pEGMA/pHEMA. Compared to pEGMA, the hydrogel character and therefore the ability to tightly bind water is reduced, leading to higher protein adsorption.(49) Yandi *et al.* established a Poly(HEMA-co-PEG_{10}) polymer showing that coatings with thicknesses larger than 10 nm showed a good resistance against nonspecific protein adsorption. Also *Ulva linza* and *Cobetia marina* settlement was reduced when thicknesses > 10 nm were tested.(50) The influence of polymer thickness on the antifouling performance was also seen in comparison to ethylene-glycols or polyglycerols of different length. (52, 53) As generally accepted reason, a good hydration seems to be the key for the inertness of the coatings which is supported by a sufficient polymer thickness that helps water to penetrate into the polymer.(49, 54)

5 Conclusions

The aim of this work was to develop a versatile platform for controlled, visible light-induced surface functionalization by polymer brushes. By using OTS as an organic monolayer and the UV-induced coupling of ITX, a functional interface was created in a controlled way that served as starting point for photo-assisted controlled surface grafting polymerization on a large range of substrates on which silanes can be assembled. The presence of the dormant ITXSP groups was shown by UV/Vis spectroscopy. The visible light-induced controlled polymerization reaction was used to prepare pHEMA brushes of different thicknesses. The reaction involves the reactivation of dormant ITXSP species to initiate the polymerization of monomers under visible light irradiation. After the successful polymerization, ITXSP had to be decoupled from the terminal end of the polymer brushes which was also proven by UV/Vis spectroscopy. In order to further exploit the light induced nature of the reaction, TEM grids were used as masks and areas of patterned polymer brushes were created. The obtained pHEMA polymers were stable in ASW and MQ water for over two weeks. Dynamic adhesion assays with diatoms showed superior fouling-release properties compared to a hydrophobic OTS monolayer, especially when greater polymer thicknesses were tested.

6 Funding Sources

The work was funded by ONR N00014-16-12979 and N00014-20-12244 as well as BMBF 02WIL1487 and the Deutsche Forschungsgemeinschaft (DFG) GRK2376/331085229.

7 Acknowledgements

The authors thank Prof. Schuhmann (Analytical Chemistry – Electroanalytics & Sensors) for access to the AFM and the SEM.

8 Abbreviations

Isopropylthioxanthone (ITX), isopropylthioxanthone-semi pinacol (ITXSP), hydroxyethyl methacrylate (HEMA), atom transfer radical polymerization (ATRP), segmented polyurethane (SPU), camphor quinone (CQ), octadecyltrichlorosilane (OTS), self-assembled monolayers (SAMs), attenuated total reflectance (ATR), Fourier transformation infrared (FTIR), atomic force microscopy (AFM), artificial seawater(ASW), contact angle (CA)

9 ORCID:

Emily Manderfeld: 0000-0002-4948-3619

Lutz Krause: 0000-0001-7531-0044

Robin Wanka: 0000-0001-8892-9399

Jana Schwarze: 0000-0001-7118-2014

Cindy Beyer: 0000-0002-3515-753X

Axel Rosenhahn: 0000-0001-9393-7190

Literature Cited

1. Doi T, Matsumoto A, Otsu T. Radical polymerization of methyl acrylate by use of benzyl N, N-diethyldithiocarbamate in combination with tetraethylthiuram disulfide as a two-component iniferter. J. Polym. Sci. A Polym. Chem. 1994; 32(15):2911–8.

2. Georges MK, Veregin RPN, Kazmaier PM, Hamer GK, Saban M. Narrow Polydispersity Polystyrene by a Free-Radical Polymerization Process-Rate Enhancement. Macromolecules 1994; 27(24):7228–9.

3. Husemann M, Mecerreyes D, Hawker CJ, Hedrick JL, Shah R, Abbott NL. Surface-Initiated Polymerization for Amplification of Self-Assembled Monolayers Patterned by Microcontact Printing. Angew. Chem. Int. Ed. 1999; 38(5):647–9.

4. Jordan R, Ulman A, Kang JF, Rafailovich MH, Sokolov J. Surface-Initiated Anionic Polymerization of Styrene by Means of Self-Assembled Monolayers. J. Am. Chem. Soc. 1999; 121(5):1016–22.

5. Yang W, Rånby B. Radical Living Graft Polymerization on the Surface of Polymeric Materials. Macromolecules 1996; 29(9):3308–10.

6. Farhan T, Huck WT. Synthesis of patterned polymer brushes from flexible polymeric films. European Polymer Journal 2004; 40(8):1599–604.

7. Gaynor SG, Matyjaszewski K. Step-Growth Polymers as Macroinitators for “Living” Radical Polymerization: Synthesis of ABA Block Copolymers. Macromolecules 1997; 30(14):4241–3.

8. Kato K. Polymer surface with graft chains. Progress in Polymer Science 2003; 28(2):209–59.

9. Miwa Y, Yamamoto K, Sakaguchi M, Shimada S. Well-Defined Polystyrene Grafted to Polypropylene Backbone by “Living” Radical Polymerization with TEMPO. Macromolecules 2001; 34(7):2089–94.

10. Tsarevsky NV, Matyjaszewski K. "Green" atom transfer radical polymerization: from process design to preparation of well-defined environmentally friendly polymeric materials. Chem Rev 2007; 107(6):2270–99.

11. Xia J, Gaynor SG, Matyjaszewski K. Controlled/“Living” Radical Polymerization. Atom Transfer Radical Polymerization of Acrylates at Ambient Temperature. Macromolecules 1998; 31(17):5958–9.

12. Ying L, Yu WH, Kang ET, Neoh KG. Functional and surface-active membranes from poly(vinylidene fluoride)-graft-poly(acrylic acid) prepared via RAFT-mediated graft copolymerization. Langmuir 2004; 20(14):6032–40.

13. Mishra V, Rajesh K. Living radical polymerization: A review. J. Sci. Res 2012; (56):141–76.

14. Allméar K, Hult A, Rårnby B. Surface modification of polymers. I. Vapour phase photografting with acrylic acid. J. Polym. Sci. A Polym. Chem. 1988; 26(8):2099–111.

15. Li Y, Desimone JM, Poon C-D, Samulski ET. Photoinduced graft polymerization of styrene onto polypropylene substrates. J. Appl. Polym. Sci. 1997; 64(5):883–9.

16. Pan X, Tasdelen MA, Laun J, Junkers T, Yagci Y, Matyjaszewski K. Photomediated controlled radical polymerization. Progress in Polymer Science 2016; 62:73–125.

17. Tasdelen MA, Uygun M, Yagci Y. Photoinduced controlled radical polymerization. Macromol Rapid Commun 2011; 32(1):58–62.

18. He D, Ulbricht M. Synergist Immobilization Method for Photo-Grafting: Factors Affecting Surface Selectivity. Macromol. Chem. Phys. 2007; 208(14):1582–91.

19. Tsujii Y, Ohno K, Yamamoto S, Goto A, Fukuda T. Structure and Properties of High-Density Polymer Brushes Prepared by Surface-Initiated Living Radical Polymerization. In: Jordan R, Advincula RC, editors. Surface-initiated polymerization. Berlin, New York: Springer; 2006. p. 1–45 (Advances in Polymer Science; 197-198).

20. Ma H, Davis RH, Bowman CN. A Novel Sequential Photoinduced Living Graft Polymerization. Macromolecules 2000; 33(2):331–5.

21. Ma H, Davis RH, Bowman CN. Principal factors affecting sequential photoinduced graft polymerization. Polymer 2001; 42(20):8333–8.

22. Boer B de, Simon HK, Werts MPL, van der Vegte EW, Hadziioannou G. “Living” Free Radical Photopolymerization Initiated from Surface-Grafted Iniferter Monolayers. Macromolecules 2000; 33(2):349–56.

23. Bai H, Huang Z, Yang W. Visible light-induced living surface grafting polymerization for the potential biological applications. J. Polym. Sci. A Polym. Chem. 2009; 47(24):6852–62.

24. Li C, Glidle A, Yuan X, Hu Z, Pulleine E, Cooper J et al. Creating "living" polymer surfaces to pattern biomolecules and cells on common plastics. Biomacromolecules 2013; 14(5):1278–86.

25. Amirzadeh G, Schnabel W. On the photoinitiation of free radical polymerization-laser flash photolysis investigations on thioxanthone derivatives. Makromol. Chem. 1981; 182(10):2821–35.

26. Balta DK, Arsu N, Yagci Y, Jockusch S, Turro NJ. Thioxanthone−Anthracene: A New Photoinitiator for Free Radical Polymerization in the Presence of Oxygen. Macromolecules 2007; 40(12):4138–41.

27. Karaca N, Karaca Balta D, Ocal N, Arsu N. Mechanistic studies of thioxanthone–carbazole as a one-component type II photoinitiator. Journal of Luminescence 2014; 146:424–9.

28. Kuluncsics Z, Perdiz D, Brulay E, Muel B, Sage E. Wavelength dependence of ultraviolet-induced DNA damage distribution: Involvement of direct or indirect mechanisms and

possible artefacts. Journal of Photochemistry and Photobiology B: Biology 1999; 49(1):71–80.

29. Zhao C, Lin Z, Yin H, Ma Y, Xu F, Yang W. PEG molecular net-cloth grafted on polymeric substrates and its bio-merits. Sci Rep 2014; 4:4982.

30. Zhu X, Ma Y, Zhao C, Lin Z, Zhang L, Chen R et al. A mild strategy to encapsulate enzyme into hydrogel layer grafted on polymeric substrate. Langmuir 2014; 30(50):15229–37.

31. Li C, Sajiki T, Nakayama Y, Fukui M, Matsuda T. Novel visible-light-induced photocurable tissue adhesive composed of multiply styrene-derivatized gelatin and poly(ethylene glycol) diacrylate. J Biomed Mater Res Part B Appl Biomater 2003; 66(1):439–46.

32. Ziani-Cherif H, Abe Y, Imachi K, Matsuda T. Visible-light-induced surface graft polymerization via camphorquinone impregnation technique. J Biomed Mater Res 2002; 59(2):386–9.

33. Magoshi T, Matsuda T. Formation of polymerized mixed heparin/albumin surface layer and cellular adhesional responses. Biomacromolecules 2002; 3(5):976–83.

34. Wang G, Chen D, Zhang L, Wang Y, Zhao C, Yan X et al. A mild route to entrap papain into cross-linked PEG microparticles via visible light-induced inverse emulsion polymerization. J Mater Sci 2018; 53(2):880–91.

35. Wang Y, Qi Y, Chen C, Zhao C, Ma Y, Yang W. Layered Co-Immobilization of β-Glucosidase and Cellulase on Polymer Film by Visible-Light-Induced Graft Polymerization. ACS Appl Mater Interfaces 2019; 11(47):44913–21.

36. Zhu X, He B, Zhao C, Ma Y, Yang W. Separated Immobilization of Incompatible Enzymes on Polymer Substrate via Visible Light Induced Living Photografting Polymerization. Langmuir 2017; 33(22):5577–84.

37. Zhu X, He B, Zhao C, Ma Y, Yang W. Simultaneously and separately immobilizing incompatible dual-enzymes on polymer substrate via visible light induced graft polymerization. Applied Surface Science 2018; 436:73–9.

38. Thome I, Bauer S, Vater S, Zargiel K, Finlay JA, Arpa-Sancet MP et al. Conditioning of self-assembled monolayers at two static immersion test sites along the east coast of Florida and its effect on early fouling development. Biofouling 2014; 30(8):1011–21.

39. Nolte KA, Schwarze J, Rosenhahn A. Microfluidic accumulation assay probes attachment of biofilm forming diatom cells. Biofouling 2017; 33(7):531–43.

40. Nolte KA, Schwarze J, Beyer CD, Özcan O, Rosenhahn A. Parallelized microfluidic diatom accumulation assay to test fouling-release coatings. Biointerphases 2018; 13(4):41007.

41. Wang M, Liechti KM, Srinivasan V, White JM, Rossky PJ, Stone MT. A Hybrid Continuum-Molecular Analysis of Interfacial Force Microscope Experiments on a Self-Assembled Monolayer. Journal of Applied Mechanics 2006; 73(5):769–77.

42. Allen NS, Catalina F, Green PN, Green WA. Photochemistry of thioxanthones—IV. Spectroscopic and flash photolysis study on novel n-propoxy and methyl, n-propoxy derivatives. European Polymer Journal 1986; 22(10):793–9.

43. Tripp CP, Hair ML. An infrared study of the reaction of octadecyltrichlorosilane with silica. Langmuir 1992; 8(4):1120–6.

44. Stenzel MH, Barner-Kowollik C. The living dead – common misconceptions about reversible deactivation radical polymerization. Mater. Horiz. 2016; 3(6):471–7.

45. Meng H, Liu L, Yang W. PMMA-containing ITX Residues and its Initiation for Synthesizing PMMA-b-PSt Copolymer. Journal of Macromolecular Science, Part A 2009; 46(9):921–7.

46. Cho J-D, Kim S-G, Hong J-W. Surface modification of polypropylene sheets by UV-radiation grafting polymerization. J. Appl. Polym. Sci. 2006; 99(4):1446–61.

47. Zhang Y, Wang H-H, Wei S, Liu J-Q, Wang W. Determination and Correlation of Solubilities of 2-Isopropylthioxanthone (ITX) in Seven Different Solvents from (299.15 to 329.85) K. J. Chem. Eng. Data 2015; 60(3):941–6.

48. Efimenko K, Finlay J, Callow ME, Callow JA, Genzer J. Development and testing of hierarchically wrinkled coatings for marine antifouling. ACS Appl Mater Interfaces 2009; 1(5):1031–40.

49. Kim S-M, Kim AY, Park H, Chun HH, Lee I, Cho Y et al. Amphiphilic Random Copolymers Consisting of Styrene, EGMA, and HEMA for Anti-Biofouling Coatings. Molecular Crystals and Liquid Crystals 2015; 622(1):151–7.

50. Yandi W, Mieszkin S, Martin-Tanchereau P, Callow ME, Callow JA, Tyson L et al. Hydration and chain entanglement determines the optimum thickness of poly(HEMA-co-PEG_{10}MA) brushes for effective resistance to settlement and adhesion of marine fouling organisms. ACS Appl Mater Interfaces 2014; 6(14):11448–58.

51. Yang W, Zhang R, Wu Y, Pei X, Liu Y, Zhou F. Enhancement of graft density and chain length of hydrophilic polymer brush for effective marine antifouling. J. Appl. Polym. Sci. 2018; 135(22):46232.

52. Schilp S, Rosenhahn A, Pettitt ME, Bowen J, Callow ME, Callow JA et al. Physicochemical properties of (ethylene glycol)-containing self-assembled monolayers relevant for protein and algal cell resistance. Langmuir 2009; 25(17):10077–82.

53. Wanka R, Finlay JA, Nolte KA, Koc J, Jakobi V, Anderson C et al. Fouling-Release Properties of Dendritic Polyglycerols against Marine Diatoms. ACS Appl Mater Interfaces 2018; 10(41):34965–73.

54. Rosenhahn A, Schilp S, Kreuzer HJ, Grunze M. The role of "inert" surface chemistry in marine biofouling prevention. Phys Chem Chem Phys 2010; 12(17):4275–86.

Table of content

Visible Light-Induced Controlled Surface Grafting Polymerization of Hydroxyethyl Methacrylate from Isopropylthioxanthone-semipinacol terminated Organic Monolayers

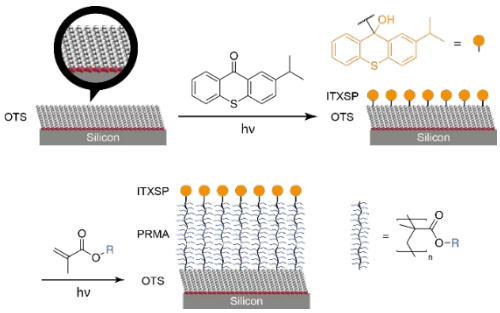

TOC-graph: Reaction scheme of the visible-light induced surface grafting polymerization on OTS using ITX as the dormant group and methacrylates as monomers (e.g. HEMA). ITX is grafted onto OTS coated silicon surfaces by exposure to UV light. Covalently coupled ITXSP groups allow to initiate a visible light induced controlled surface grafting polymerization of methacrylate polymers.